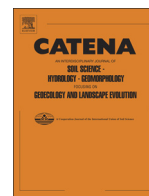




Contents lists available at ScienceDirect

Catena

journal homepage: www.elsevier.com/locate/catena

High variability of soil erosion and hydrological processes in Mediterranean hillslope vineyards (Montes de Málaga, Spain)



J. Rodrigo Comino ^{a,d,*}, J.D. Ruiz Sinoga ^d, J.M. Senciales González ^b, A. Guerra-Merchán ^c, M. Seeger ^a, J.B. Ries ^a

^a Department of Physical Geography, Trier University, Behringstrasse, D-54286 Trier, Germany

^b Department of Geography, Málaga University, Campus of Teatinos s/n, 29071 Málaga, Spain

^c Department of Ecology and Geology, Málaga University, Campus of Teatinos s/n, 29071 Málaga, Spain

^d Instituto de Geomorfología y Suelos, University of Málaga, 29071, Málaga, Spain

ARTICLE INFO

Article history:

Received 8 January 2016

Received in revised form 27 April 2016

Accepted 8 June 2016

Available online xxxx

Keywords:

Vineyards

Soil erosion

Runoff

Guelph permeameter

Rainfall simulation

ABSTRACT

Conventional Mediterranean vineyards from the Montes de Málaga (Axarquía region, Spain) are characterized by high average temperatures, extreme rainfall events during autumn and winter, elevated stoniness and steep slopes (20–50°). Traditionally, several problems of high soil loss, rill and ephemeral gully generation, and elevated runoff are observed by farmers, which are increasing land degradation processes and a decrease of the productivity.

According to this, the main aims of this paper were: i) to quantify the initial soil loss, surface flow and infiltration processes; ii) to characterize and describe the hydrological and geomorphological dynamics; iii) to detect the key factors, which control the soil erosion processes.

For this purpose, a combined methodology was applied, using soil analysis, a small portable rainfall simulator and a Guelph permeameter on one experimental plot cultivated with vineyards with steep slopes. Results showed a high variability of soil erosion and permeability processes. Soil analysis showed an elevated concentration of silt particles and stoniness, with higher contents of sand particles between 0 and 5 cm, and clays from 5 cm. With a Guelph permeameter, high average of permeability and saturated hydraulic conductivity with elevated standard deviation were observed. Furthermore, an increase of these parameters from the upper to the foot slope was registered. By using rainfall simulations, on the upper and the foot slope positions the highest runoff coefficient and soil loss were registered. The most elevated peak of sediment concentration was obtained on the middle slope. In general, high infiltration coefficients between 66.5 and 100% were observed.

In conclusion it was observed that the activation of the soil erosion processes was due to the distribution of the surface soil components (high roughness, several cracks and high stoniness and silt content), the steep slopes and the impact of the soil traditional tillage practices. These Mediterranean hillslope vineyards registered a mixed Hortonian-Hewlettian model, which combines surface and sub-surface flow conditioned by the micro-topographical changes and its saturation degree.

© 2016 Elsevier B.V. All rights reserved.

1. Introduction

Mediterranean hillslope vineyards are one of the most altered eco-geomorphological systems in south Europe. Vaudour et al. (2015) reported that in the last ten years several studies have been carried out to evaluate soil erosion processes in traditional European viticulture areas of France, Spain or Italy. Numerous authors claimed that the extreme rainfall events, the steep slopes, the intensive soil tillage practices and the soil surface components could be the most relevant indicators to analyse and classify actual soil erosion processes for these areas. In some Mediterranean vineyards, due to extreme land degradation has

been registered an increase of the risk of catastrophic floods combining high surface flows and sediment transports (Ramos and Martínez-Casasnovas, 2006).

Along the Mediterranean pluviometric gradient from Murcia region to Andalusian southeast coast (Spain) the climatic conditions (high average temperature and evapotranspiration values, and extreme rainfall events) can be more extreme and extend this erosive dynamic (Ruiz-Sinoga et al., 2011; Ruiz-Sinoga et al., 2010; Ruiz-Sinoga and Romero-Díaz, 2010; Ruiz-Sinoga and Martínez-Murillo, 2009a, 2009b). The vineyards of the Axarquía region in the Montes de Málaga (Málaga, Spain), where the recognized Moscatel and Pedro Ximénez grapes are produced (Haba, 1997; Padilla-Monge, 2001), are one of the most popular agricultural activities developed in this semi-arid environmental context.

* Corresponding author.

E-mail address: sj6rodr@uni-trier.de (J. Rodrigo Comino).

In this area, the degradation of soil chemical and physical properties, the soil erosion rates and the hydrological dynamics had been reported by photography, parametrical techniques as USLE (Universal Soil Loss Equation) or GIS by regional studies and were supposed to be very high (Blanco-Sepúlveda and Gómez Moreno, 2006; Blanco-Sepúlveda and Larrubia-Vargas, 2008; Blanco-Sepúlveda and Senciales-González, 2001a, 2001b; Justicia-Segovia, 1988; Martínez-Murillo and Senciales-González, 2003; Ruiz-Sinoga, 1987; Senciales-González and Rodrigo-Comino, 2011); however they were not measured directly *in situ*. Regarding to this bibliography, it is clear that there is missing a serious data base on soil erosion processes with field measures of this region. *In situ* measurements are really necessary to know exactly how the land management agents and farmers must proceed against the land degradation processes. Following these researches, the land degradation processes are due to principally four causes: i) concentrated heavy rainfall events within no >30 days per year; ii) steep slopes (26–76%); iii) high stoniness (>40%); iv) traditional soil tillage of the wine growers, composed by the removing vegetation cover under and around the vines. As a consequence of these tillage practices and the extreme environmental conditions, soil erosion problems have been observed since the Muslim ages in the Middle Age (Padilla-Monge, 2001; Quintana-Toret, 1985; Ruiz-Sinoga, 1987). Nowadays, there is an elevated awareness of the decreasing of the grape production, the development of cheap protection measures, the problems by soil losses after extreme rainfall events or the difficulties in soil water retention capacity by public organisms, local press and farmers.

Historically, in some places vine growers have taken measures against soil erosion, such as building rills, in order to canalize the surface flow and small walls of stones to reduce soil loss. However, often, these traditional protection measures are not enough, because nowadays the high soil losses and excess surface flow continue the land degradation processes. The combination between rural techniques and new methods on soil science must become indispensable. So, this research was carried out following a main quantitative aim and two concrete qualitative purposes: i) to quantify the initial soil loss, surface flow and infiltration processes; ii) to characterize and describe the hydrological and geomorphological dynamics; iii) to detect the key factors, which control the soil erosion processes.

2. Material and methods

2.1. Study area

The experimental study site is located (Fig. 1) in the village of Almáchar, which is situated in the Axarquía region in the Montes de Málaga relief (Andalucía, Spain).

2.1.1. Geological context

From a geological point of view, the study area is located in the “Benamocarra unit” within the Internal Zone of the Betic Cordillera (Estévez-González and Chamón, 1978). Tectonically this unit is located on materials of the Alpujarride complex and under materials of the complex Malaguide. In general, this monotonous unit is composed of Palaeozoic dark schists, with approximately 700 m thickness. Estévez-González and Chamón (1978) describe two different facies: i) mica schists with well-developed schistosity, small garnets (1–2 mm) and intercalations of lenticular levels of white quartz and; ii) quartz mica schists without garnets, which have less developed the schistosity, showing higher resistance than the first facies. These types of rocks are predominant along the eastern part of the studied area, especially in its upper part, characterized by a large number of rocky outcrops and slights. In general, these rocks have been subjected to intense deformation as testifies the axial schistosity axial-plane linked to isoclinal folds and the abundant fractures of different scales.

The schistosity shows an orientation which varies between N-S with dips of 40°–55° W and N140–165E with dips of 40–65° SW. Fractures have a variable orientation: i) N/NE to S/SW with dips between 55 and 85°E; ii) NW-SE with dips of 66–75°SW; iii) little signals of E-W with dips of 70–80°S.

2.1.2. Climatic and land management contexts

The annual average rainfall depth is 520 mm and its highest concentration is distributed between October and January (78%) in a few extreme events, but with a high inter-annual variability. For example, since September until November in 2014 was collected a total rainfall of 343.6 mm, which 200.6 mm were obtained in only one event of

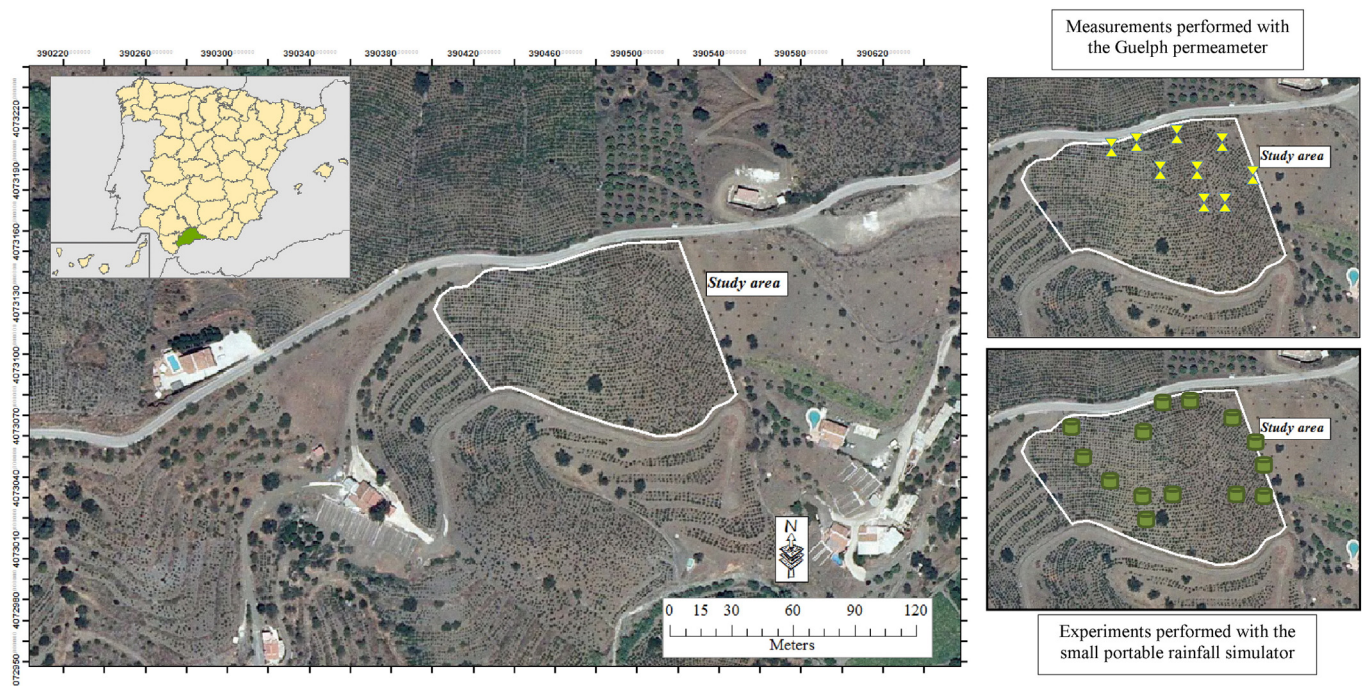


Fig. 1. Study area and location of the measurements and experiments.

two days. In 2015, since September until November, the total amount was reduced arranging 189.4 mm. In summer, between June and August, only a 4% of the total average rainfall depth is registered. In the study area, during May, June, July and August (in 2014 and 2015) did not register any precipitation. The annual average temperature is 17.2 °C, with maximum average values in July and August (24.5–24.9 °C) and minimum average values in December, January and February (11.3–11.5 °C).

The experimental plot is characterized by a conventional and traditional grape production with an irregular distribution of the marc of plantation along with high hillslopes (20–50°). Several changes have been registered in the actual landscape due to the economic crisis of the viticulture sector, increasing abandoned lands and, with the insertion of new plantations of mango (*Mangifera indica*) and avocado (*Persea americana*) (Rodrigo-Comino, 2014; Rodrigo-Comino and Senciales-González, 2015).

The main variety of grape is *Muscat of Alexandria*, registered by a Spanish DO (Designation of Origin) with the name: “Málaga, Sierras de Málaga and Padas de Málaga”. The 2014 and 2015 harvest was carried out at the beginning of July, due to the highest temperatures and the fast maturation of the grapes.

The land management is characterized by: i) soil tillage with hoes and shovels before (April–May) and after vintage (October–December); ii) the application of herbicides to avoid the competence of water with another plants (November–December); iii) the utilisation of animals to recollect the grape production; and iv) the application of natural and organic soil amendments of domestic cows and goats (February–March).

Historically, due to the steep soil erosion problems by the concentrated rainfall events and the steep slopes, the vine growers have developed rudimental protection measures in some places. The first protection measure is the “sangría” or “desaguadero”, composed by anthropic handmade rills, which collect and interrupt the surface flow and canalize the water directly to another principal rill. The second traditional technique are stony walls (“albarrada” or “balate”) situated along the upper slope to contain the soil across the slope. This second protection measure is included in the experimental area of this research.

2.2. Soil analysis

The soil samples were collected during July and August of 2014 on the experimental area from three different slope positions (upper, middle and foot), two depths (0–5 cm and 5–15 cm) along inter-rows and under the vines and with three replicates (in total 36 samples, taking about 3–4 kg per sample). After sieving (<2 mm), different parameters were analysed in the laboratory in order to determine: texture, bulk density, total organic carbon, carbonates, electrical conductivity, pH and soil water content.

Grain particle size between 0.004 mm and 2 mm was measured with a Coulter LS230, by combining different diffraction patterns of a light beam. 1 cm³ steel cylinders were used to calculate the bulk density with undisturbed soil samples.

The total of organic carbon was measured by weight difference, applying 430 °C (24 h) in a muffle furnace (Davies, 1974; Rosell et al., 2001). Electrical conductivity was measured by a digital conductivity-meter and carbonates with a Bernard calcimeter. pH was obtained in distilled water and KCl with a digital pH-meter with a relation of 1:5. Differences bigger than 1 between values of pH with H₂O and pH with KCl show the soil acidification trend. All these chemical parameters were analysed by their relations with salinity, texture, clay mineralogy, moisture content, ionic strength, temperature and bulk density properties (Gruber and Kosegarten, 2002; Jackson, 2014; Lesch and Corwin, 2003; Taylor et al., 2009).

Water-holding characteristics were calculated with a pressure plate extractor, corresponding to the field capacity (%) and the permanent wilting point (%), respectively.

Finally, three soil profiles were described to classify the type of pedon, using the methodology of FAO-WRB (IUSS Working Group WRB, 2014, 2007, 2006) and regional bibliography (Aguilar-Ruiz et al., 1993; Rodrigo-Comino, 2014).

2.3. Field-measures of permeability, saturated hydraulic conductivity and soil matrix flux potential

Several authors claimed that field measurements of the infiltration, the permeability and the hydraulic conductivity (K_f) provide more representative data than the laboratory measures (Kumar et al., 2010; Rienzner and Gandolfi, 2014). This is related to the possible influence of the small cracks and macro-pores of the soil aggregates (Bodhinayake and Cheng Si, 2004; Buczko et al., 2006).

A large number of instruments and methods are available to measure the infiltration, the permeability and K_f (Archer et al., 2013; Bagarello et al., 2014; Cerdà, 1997; Gupta et al., 2006, 1993; Gwenzi et al., 2011; Huang et al., 2016, 2014; Jačka et al., 2014; Kodešová et al., 2010; MacDonald et al., 2012; Peter and Ries, 2013; Wu et al., 1992). In this research, a Guelph permeameter (GP) was applied. Through a modified Mariotte bottle device, the GP (Fig. 2.1) sends a constant water level discharge three-dimensionally into a small cylindrical bore-hole (Erick et al., 1989; Erick and Reynolds, 1992; Reynolds and Erick, 1987; Reynolds and Lewis, 2012). Each experiment in the field was carried out by following the designed protocol by (Rodrigo-Comino et al., 2016b): i) the standard procedure to prepare the permeability well was performed by following the recommendations of the Guelph permeameter manual (Soil moisture Equipment Corp, 2008); ii) two measurements for the same borehole (between 10–25 cm depth and



Fig. 2. Guelph permeameter and rainfall simulator.

Table 1
Soil analysis.

ID* (n = 3)	Gravel (%)	Sand (%)	Silt (%)	Clay (%)	BK (gcm ⁻³)	TOC (%)	CaCO ₃ (%)	EC (ds/m)	pH (H ₂ O)	pH (KCl)	Dif.	SWC (FC)	SWC (WP)
U 0–5	55.7 ± 2.4	25.7 ± 0.2	68.2 ± 0.5	6.1 ± 0.5	1.5 ± 0.1	3.4 ± 0.3	1 ± 0.3	0.1 ± 0.01	7.3 ± 0.03	5.5 ± 0.01	1.8	21.9 ± 0.7	7.8 ± 0.5
U 5–15	49.9 ± 0.6	26 ± 0.4	67.9 ± 0.4	6 ± 0.3	1.5 ± 0.1	3.0 ± 0.5	0.8 ± 0.3	0.04 ± 0.01	7.4 ± 0.01	5.2 ± 0.01	2.2	22.3 ± 0.7	7.7 ± 0.3
UV 0–5	62.4 ± 1.9	19.5 ± 0.5	75.4 ± 0.9	5.5 ± 0.2	1.5 ± 0.1	2.4 ± 0.4	0.8 ± 0.4	0.1 ± 0.01	7.2 ± 0.03	5.2 ± 0.01	1.9	22.7 ± 0.6	7.6 ± 0.7
UV 5–15	53 ± 0.7	19.5 ± 0.4	74.4 ± 1.2	6 ± 0.2	1.4 ± 0.1	2.6 ± 0.5	0.9 ± 0.2	0.1 ± 0.04	7 ± 0.01	5.2 ± 0.01	1.8	23.2 ± 1	8.0 ± 0.6
M 0–5	53.9 ± 0.4	14.9 ± 0.2	79.5 ± 0.4	5.8 ± 0.3	1.5 ± 0.1	3.2 ± 0.4	0.7 ± 0.3	0.2 ± 0.03	6.8 ± 0.03	5.4 ± 0.01	1.4	25.0 ± 1.6	7.6 ± 0.8
M 5–15	50.9 ± 0.6	12.5 ± 0.2	81.6 ± 0.3	6 ± 0.2	1.5 ± 0.04	2.9 ± 0.6	1 ± 0.3	0.1 ± 0.01	6.9 ± 0.02	5 ± 0.01	1.9	23.7 ± 1.2	8.7 ± 0.3
MV 0–5	63.5 ± 2	31.2 ± 0.5	63.9 ± 1.3	4.8 ± 0.2	1.5 ± 0.1	3.9 ± 0.2	0.7 ± 0.2	0.1 ± 0.02	7 ± 0.03	5.5 ± 0.01	1.5	25.3 ± 1.3	8.4 ± 0.5
MV 5–15	58.3 ± 1.5	30.3 ± 1.4	64.6 ± 1.2	5.1 ± 0.4	1.5 ± 0.03	3.7 ± 0.3	0.7 ± 0.1	0.1 ± 0.02	6.9 ± 0.01	5.1 ± 0.01	1.8	24.9 ± 0.7	8.3 ± 0.6
F 0–5	52.8 ± 1.9	29.1 ± 1.4	66.0 ± 2.4	4.8 ± 0.3	1.5 ± 0.1	3.0 ± 0.5	0.9 ± 0.3	0.1 ± 0.1	7.1 ± 0.03	5.7 ± 0.01	1.4	26.9 ± 0.5	7.2 ± 0.3
F 5–15	49.2 ± 0.9	20.8 ± 0.8	73.7 ± 1.8	5.6 ± 0.5	1.4 ± 0.1	2.9 ± 0.5	0.9 ± 0.3	0.1 ± 0.01	7.2 ± 0.02	5.3 ± 0.01	1.9	26.9 ± 0.5	7.2 ± 0.4
FV 0–5	51.4 ± 1.3	23.6 ± 0.9	70.8 ± 1.4	5.6 ± 0.3	1.5 ± 0.1	3.1 ± 0.4	0.9 ± 0.1	0.1 ± 0.02	7 ± 0.03	5.5 ± 0.01	1.5	24.7 ± 1.6	6.6 ± 0.2
FV 5–15	51.8 ± 1.1	13.3 ± 0.2	80.8 ± 0.6	5.9 ± 0.3	1.5 ± 0.2	2.7 ± 0.5	0.9 ± 0.2	0.1 ± 0.01	7.3 ± 0.01	5.2 ± 0.01	2.1	23.7 ± 1.7	6.9 ± 0.2

ID* = U: upper slope; M: middle slope; F: foot slope; 0–5: cm depth; 5–15: cm depth; V: under vines. BK: bulk density; TOC: total organic content; CaCO₃: carbonates content; EC: electrical conductivity; Dif: difference between pH (H₂O) and pH (KCl); SWC (FC): soil water content (field capacity); SWC (WP): soil water content (wilting point). In black color, the cells with the most relevant values were indicated.

4–10 cm radius) were carried out, the first was with 5 cm water level in well and the second one with 10 cm; iii) the total duration for each measurement was 30 min or when the principal reservoir reached the total emptying (76 mm); iv) the observations must be recollected every 2 min, measuring the time with a digital stopwatch; v) steady rates (cm min⁻¹) were calculated with the average of the total measurements. Final results with the GP will show the hydrodynamic processes between 10 and 25 cm depth of soil in mm h⁻¹.

Nine experiments were realized with three repetitions at different slope positions of the studied area (upper, middle and foot). Finally, with the obtained results were calculated the permeability rate (1), the K_fs (2) and the soil matrix flux potential (3) (Reynolds, 1986; Reynolds and Elrick, 2002; Rodrigo Comino et al., 2016b; Zhang et al., 1998):

$$\text{Permeability rate} = \left(\frac{y * Q1}{2\pi(\alpha * H1)} \right) * 60 \text{ [mm h}^{-1}\text{]} \quad (1)$$

$$Kf_s = \left(\frac{C1 * Q1}{2\pi H1^2 + \pi a^2 C1 + 2\pi \left(\frac{H1}{\alpha} \right)} \right) * 600 \text{ [mm h}^{-1}\text{]} \quad (2)$$

$$\phi = \left(\frac{C1 * Q1}{(2\pi H1^2 + \pi a^2 C1) \alpha + 2\pi(H1)} \right) * 6000 \text{ [mm}^2 \text{ h}^{-1}\text{]} \quad (3)$$

- C1 = shape factor
- y = area of the combined reservoir (35.22 cm²)
- Q1 = quasi-steady flow rate out of the permeameter and into the soil (cm min⁻¹)
- H1 = the first head of water established in borehole (cm)
- α = macroscopic capillary length parameter
- a = borehole radius (cm).

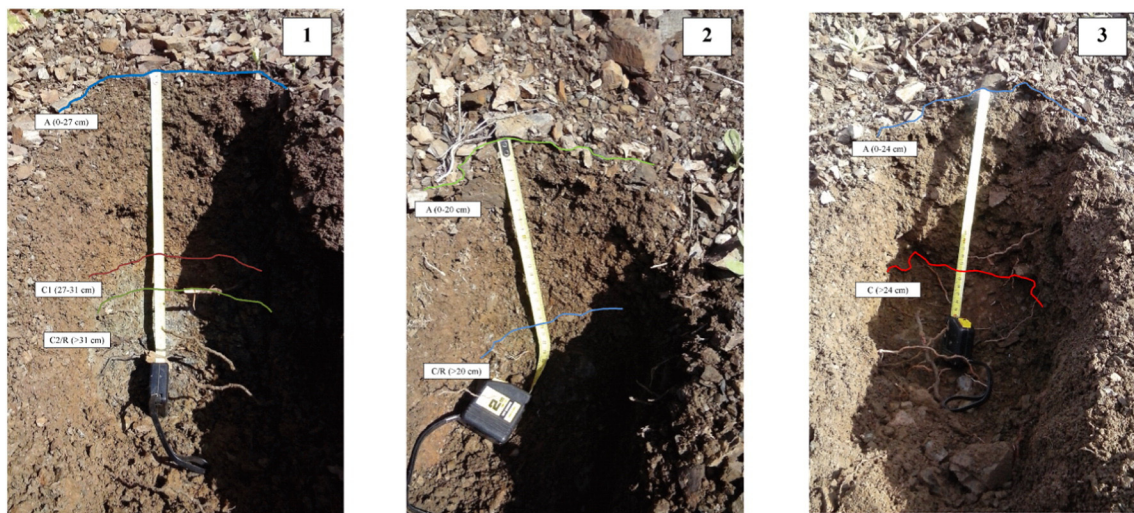


Fig. 3. Soil profiles along the experimental plot: upper (1), middle (2) and foot (3) slope.

Table 2
Spearman's rank correlations coefficient for all the soil samples.

	Gravel	Sand	Silt	Clay	BK	TOC	CaCO ₃	EC	pH (H ₂ O)	pH (KCl)	Dif.	SWC (FC)	SWC (WP)
Gravel		0.36	-0.33	-0.36	0.1	0.35	-0.44	0.6*	-0.3	0.2	-0.37	-0.05	0.38
Sand			-0.99**	-0.47	-0.21	0.64*	-0.34	0.35	0.16	0.38	-0.3	0.25	0.15
Silt				0.43	0.27	-0.65*	0.32	-0.34	-0.13	-0.36	0.34	-0.25	-0.18
Clay					0.46	-0.16	0.49	-0.5	0.26	-0.41	0.47	-0.77**	0.13
BK						-0.02	0.32	-0.17	0.48	0.04	0.43	-0.68*	-0.18
TOC							-0.25	0.6*	-0.25	0.28	-0.46	0.22	0.36
CaCO ₃								-0.22	0.2	0.17	0.02	-0.33	-0.17
EC									-0.6*	0.63*	-0.88**	0.43	0.08
pH (H ₂ O)										0.12	0.64*	-0.34	-0.48
pH (KCl)											-0.62*	0.42	-0.48
Dif.												-0.57	-0.1
SWC (FC)													-0.21
SWC (WP)													

* $p < 0.05$; ** $p < 0.01$. BK: bulk density; TOC: total organic content; CaCO₃: carbonates content; EC: electrical conductivity; Dif: difference between pH (H₂O) and pH (KCl); SWC (FC): soil water content (field capacity); SWC (WP): soil water content (wilting point). In black color, the cells with the highest values were indicated.

2.4. Rainfall simulations

Soil loss, runoff, sediment concentration and infiltration rates were calculated using a small portable rainfall simulator. Rainfall simulations (Fig. 2.2) is a nozzle type simulator, based on the one designed by Cerdà (1998a, 1998b, 1999), Lasanta et al. (2000) and calibrated by Ries et al. (2009). Finally, it has been modified and described in detail by Iserloh et al. (2012). The major parts of the rainfall simulator are a square metal frame (0.45 m × 0.45 m) with one nozzle (Lechler 460 608), four telescopic aluminium legs in order to position the nozzle at a height of two meters above the plot. During rainfall experiments, the aluminium linkage is covered by a rubber tarpaulin to avoid wind influences. The test plot is circular, with a diameter of 60 cm and an area of approximately 0.28 m². The plot outlet is V-shaped and placed at the deepest point of the plot at surface level. With a flow control and a 12 V low-pressure bilge pump, a controlled and reproducible simulated rainfall can be adjusted. The rainfall simulator was calibrated by Iserloh et al. (2013a, 2013b) for a rainfall intensity of 40 mm h⁻¹.

Test duration per rainfall simulation was 30 min on upper, middle and foot slope. Before the beginning of the experiments, slope (°), vegetation and stone cover (%) and, roughness (%) with the chain method (Saleh, 1993) were measured. During the experiment, runoff with eroded material was collected in plastic bottles. The 30 min of the different experiments were partitioned into six measuring intervals of five minutes duration. At the beginning of a new interval, the bottles were changed. The amount of runoff was measured gravimetrically for each bottle.

The collected water with sediments in each bottle was filtrated separately with circular fine-meshed filter papers (Munktell©, Prod.-Nr. 3.104.185, <2 µm mesh-width). The filters were dried to constant weight at 105 °C and weighted thereafter for determining suspended sediment load (SSL). Finally it is possible to calculate runoff, suspended sediment concentration (SSC) and infiltration rate.

Table 3
Localisations and sizes of the bore holes, and final steady rates.

Slope position	Slope (°)	Depth hole	Radius (cm)	R1 (cm min ⁻¹)*	R2 (cm min ⁻¹)**
Upper	6	23	6.5	0.06 (0.05)	0.07 (0.07)
	6	18.5	5.5	0.07 (0.08)	0.42 (0.08)
	12	21	8	0.02 (0.04)	2.63 (1.24)
Middle	21	17.5	6.5	0.14 (0.06)	2.34 (0.71)
	18	16	4	0.08 (0.02)	0.46 (0.56)
	12	15.5	7	0.07 (0.25)	0.76 (0.2)
Foot	5	15	5	0.08 (0.24)	3.87 (0.93)
	14	15	5	0.03 (0.04)	2.12 (0.42)
	8	11	12	0.25 (0.3)	5.28 (0.26)

* 5 cm of the head of water.

** 10 cm of the head of water.

3. Results

3.1. Soil analysis

The results of chemical and physical analysis are shown in Table 1. Although the average values are similar, materials bigger than 2 mm were predominant along the upper and middle slope (>55%), under the vines (56.7%) and between 0 and 5 cm depth (56.59%). The textural analysis of the fine earth fraction showed that the highest percentage of size particles was the silt fraction (72.2%). All the studied samples have a texture silt loam, except the samples on the inter-rows of the middle slope and under the vines between 5 and 15 cm depth, whose texture is silt. The other registered fractions were 22.2% (sand) and 5.6% (clays). The maximum content of silt (≈80%) was noted along the middle and foot slope (under vines and between 5 and 15 cm). The highest concentration of sand particles was located along the middle slope and under vines (≈30%). Electrical conductivity values were very low (0.1 dS m⁻¹), not showing problems by salinity content. Bulk density and carbonates not showed any differences in all the study area (about 1.5 g cm⁻³ and <1% respectively).

A total organic content of 2.9% for the upper and foot slopes were determined. 2.4% for the upper slope and 2.6% for the under vines were the lowest percentage in the study area. On the other part, the highest values (3.4%) were observed in the middle slope.

For all the samples, the differences of pH showed a high trend of soil acidification. The highest values could be observed along the upper slope (between 1.8 and 2.2). On the other hand, the middle and the foot slopes registered the lowest values (between 1.4 and 2.1).

The highest points of field capacity were measured at the foot slope (26.9%) and the lowest on upper slope (21.9–23.2%). The permanent wilting point varied with minimal differences: i) 6.6 and 6.9% along the foot slope under the vines and; ii) maximum values between 8.3% and 8.7% for the middle slope under the vines.

Finally, *Leptosol eutric* was classified using the methodology of FAO-WRB classification (Fig. 3). The *Leptosol* was characterized by AR stoniness horizon type with maximum depths of 30 cm. The *eutric* WRB qualifier was confirmed after revising the regional soil maps and bibliography (Aguilar-Ruiz et al., 1993; Rodrigo-Comino, 2014).

Finally, the Spearman's rank correlation coefficients for all collected soil samples, on the inter-rows and rows, and at 0–5 and 5–15 cm depth were added.

In general (Table 2), high correlations at the 0.01 statistical significance level were observed between the sand and silts content (−0.99), electrical conductivity with differences of pH, and SWC (FC) with clay particles (−0.77). Relationships at the 0.05 level were noted between the bulk density and the soil water content in field capacity (−0.68), and the sand and the silt particles with the total organic content (0.64 and −0.65 respectively).

Table 4
Results of measurements using the Guelph permeameter.

Slope position	Inf. rate (mm h ⁻¹)	Kf _s (mmh ⁻¹)	Φ (mm ² h ⁻¹)
Upper	26.05 (26.75)	9.01 (9.52)	4.17 (4.41)
Middle	37.75 (26.03)	11.62 (9.96)	5.38 (4.61)
Foot	94.54 (36.19)	32.32 (10.63)	14.96 (4.92)
Total average (n = 9)	52.78 (36.6)	17.65 (14.07)	8.17 (6.52)

3.2. Field-measurements of permeability rate, saturated soil hydraulic conductivity and soil matrix flux potential

Nine measurements using the GP were performed at three different parts of the experimental area: upper, middle and foot slope. The registered inclination was between 5 and 21° and the soil moisture between 0.5 and 1.5%.

Firstly, the steady rates into the Guelph permeameter for 5 cm (R1) and 10 cm (R2) of the head of water were obtained (Tables 3 and 4). This value only indicates the velocity of the water inside the GP in cm min⁻¹. This initial data will be the most important value to calculate the final rates, saturated hydraulic soil conductivities and soil matrix flux potentials. Results showed several differences for each point with high standard deviations. Values arranged between 0.02 cm min⁻¹ to 0.25 cm min⁻¹ with 5 cm of the head of water, and between 0.07 ± 0.704 cm min⁻¹ and 5.28 cm min⁻¹ for 10 cm of the head of water.

Permeability rates (mm h⁻¹) were calculated in the study area per intervals of 2 min for 5 cm, 10 cm and their average of the head of water. Results were represented using box plot graphics (Fig. 4).

The highest peaks were observed in the measurements with 10 cm of head of water. It can be registered that the most variable permeability rates were founded between the intervals 2 and 4 min. From this point,

the steady rate starts to decrease to the final of the measurement. Furthermore, in five out of nine measurements using 10 cm, the GP was empty before 30 min (between the intervals of 14–28 min), showing peaks >200 mm h⁻¹.

Total average values showed a decrease from 81.8 mm h⁻¹ (at the beginning) to 11.8 mm h⁻¹ (last interval), with a linear trend of R² = 0.95.

In general, all measurements obtained a high standard deviation due to the great variability of the final results. The GP measures showed an increasing of the permeability rates and Kf_s along the slope: i) upper: 26.05 mm h⁻¹ and 9.01 mm h⁻¹; ii) middle: 37.75 mm h⁻¹ and 11.62 mm h⁻¹ and; iii) foot: 94.54 mm h⁻¹ and 32.32 mm h⁻¹. The Φ increased parallel to the Kf_s. The results showed the highest values along the foot slope (14.96 mm² h⁻¹) and a total average of 8.17 mm² h⁻¹.

3.3. Rainfall simulations

Fourteen rainfall simulations were performed at three different heights of the study area (Table 5 and Fig. 5): i) upper slope: n = 5; middle slope: n = 4 and; foot slope: n = 5.

Environmental plot characteristics showed slope values between 15° and 42°, a vegetation cover lower than 10%, a high stone cover (>80%), and a roughness between 2% and 7%.

In general, just any runoff during the first five minutes was not obtained (it occurred only on the foot slope position). After that, the values were increasing until the last interval. According to this, high infiltration coefficients close to 100% were registered. Furthermore, the highest soil loss (4.8 g) and sediment concentration (66.95 g L⁻¹) values were obtained during the last two intervals (both on the upper slope), coinciding with the most elevated peaks of runoff (72.4%).

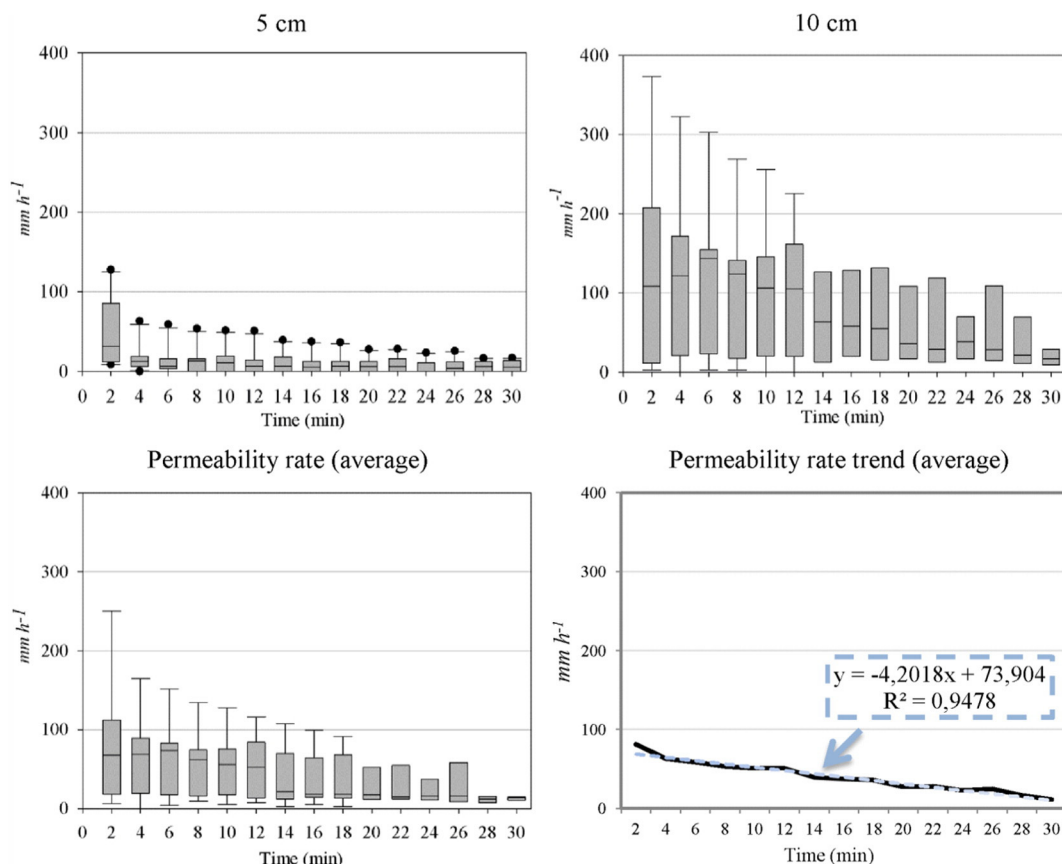
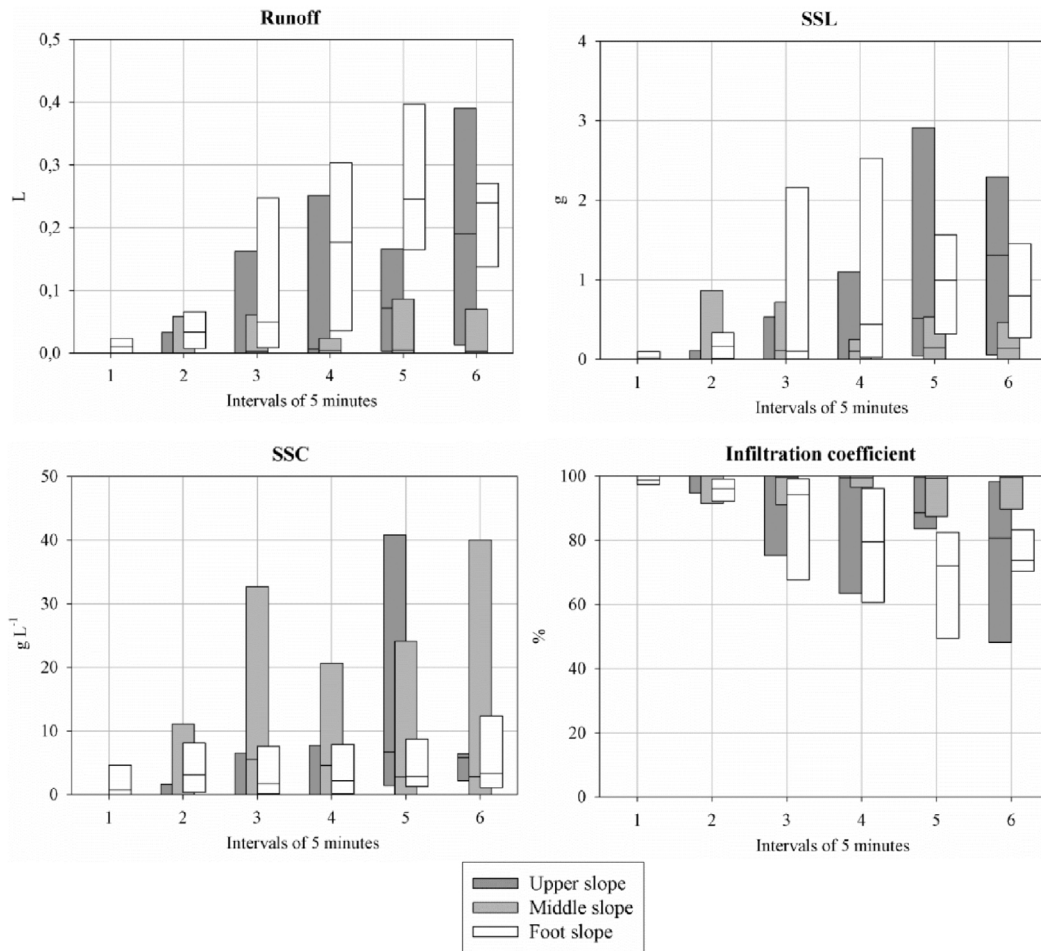


Fig. 4. Permeability rates (mm h⁻¹) for 5 cm, 10 cm, total average of head of water and linear trend of the average permeability rates.

Table 5
Results of rainfall simulations experiments per slope position.

Slope position	Runoff		SSL		SSC	Infiltration	Runoff coefficient	Infiltration coefficient	Slope	Vegetation cover	Stone cover	Roughness
	L	L m ⁻²	g	g m ⁻²	g L ⁻¹	mm h ⁻¹	%	%	°	%	%	%
Upper	0	0	0	0	0	31.29	0	100	26	5	95	5.3
	1.27	4.53	8.94	31.93	7.05	22.47	33.6	66.5	38	0	93	3.7
	0.03	0.12	0.20	0.73	6.19	32.88	0.7	99.3	15	3	85	6.7
	0.51	1.83	2.44	8.70	4.77	42.75	8.2	91.8	39	3	95	2.5
	0.49	1.76	4.34	15.48	8.78	40.24	8.4	91.6	34	10	80	2
Average	0.5 ± 0.5	1.6 ± 1.8	3.2 ± 3.7	11.4 ± 13.1	6.9 ± 3.3	33.9 ± 8	10.2 ± 13.7	89.8 ± 13.7	30.4 ± 10	4.2 ± 3.7	89.6 ± 6.8	4 ± 2
Middle	0	0	0	0	0	40.71	0	100	31	5	85	3.5
	0.39	1.39	3.44	12.28	8.84	27.75	9.5	90.5	36	2	95	8
	0	0	0	0	0	29.14	0	100	42	3	95	3
	0.03	0.1	1	3.59	34.41	31.18	0.7	99.3	30	3	85	6.8
	Average	0.1 ± 0.2	0.37 ± 0.7	1.11 ± 1.6	3.97 ± 5.8	10.62 ± 16.3	32.2 ± 5.8	2.6 ± 4.7	97.5 ± 4.7	34.75 ± 5.5	2.6 ± 0.5	90 ± 5.8
Foot	0.81	2.9	2.5	8.94	3.08	32.67	16.3	83.7	29	7	85	5.4
	0.17	0.62	1.54	5.49	8.8	29.02	4.2	95.8	25	5	90	3.3
	0.8	2.86	0.66	2.34	0.82	36.57	14.5	85.5	35	2	90	4.6
	0.4	1.43	2.6	9.28	6.5	41.43	6.7	93.3	16	3	95	2.2
	1.21	4.33	9.33	33.33	7.7	28.24	26.6	73.4	30	3	85	6.8
	Average	0.7 ± 0.4	2.4 ± 1.4	3.3 ± 3.5	11.9 ± 12.3	4.89 ± 3.3	33.6 ± 5.5	13.6 ± 8.8	86.4 ± 8.8	30.4 ± 7.1	4.3 ± 2	90 ± 4.2
Total average	0.4 ± 0.4	1.6 ± 1.6	2.6 ± 3.1	9.4 ± 11	6 ± 8.6	33.3 ± 6.1	9.2 ± 10.4	90.8 ± 10.4	30.4 ± 8	3.7 ± 2.5	89.5 ± 5.2	4.6 ± 2

S.



*SSL: suspended sediment load; SSC: suspended sediment concentration.

Fig. 5. Rainfall simulation results per intervals on different slope positions.

On the upper slope, any surface flow was not observed during the first 5 min (infiltration of 100%). After that, runoff coefficients per intervals increased with maximum values of 72.4%. Total average soil loss was 3.2 g ($11.4 \text{ g}^{-1} \text{ m}^{-2}$) and the runoff ranged 0.5 L ($1.6 \text{ L}^{-1} \text{ m}^{-2}$). The mean value of sediment concentration was 5.4 g L^{-1} and the infiltration rates arranging 33.9 mm h^{-1} , which supposed a total average infiltration coefficient of 89.8%.

On the middle slope, neither any surface flow during the first interval was observed. From this point, low values of runoff and soil loss were reported. Total average soil loss during the experiments ranged to 1.11 g ($3.97 \text{ g}^{-1} \text{ m}^{-2}$). On the other hand, total average runoff was the lowest ranged 0.1 L ($0.37 \text{ L}^{-1} \text{ m}^{-2}$). However, the sediment concentration was higher than in the upper slope with an average of 10.81 g L^{-1} . 32.2 mm h^{-1} was the total registered average infiltration rate, supposing an increasing respect to the upper slope position (97.5% of infiltration coefficient).

Runoff on the foot slope position started since the first interval until reaching maximum values of 57.1%, registered at the interval from 20 to 25 min. The total average of suspended sediment load was 3.3 g ($11.9 \text{ g}^{-1} \text{ m}^{-2}$) and the runoff 0.7 L ($2.4 \text{ L}^{-1} \text{ m}^{-2}$). According to this, the sediment concentration obtained the lowest values arranging 4.9 g L^{-1} . Finally, infiltration rates showed high values (33.6 mm h^{-1}), which supposed 86.4% of infiltration coefficient.

4. Discussion

High variability of hydrological and soil erosion processes have been showed during this research for one experimental area at three different slope positions. A combined methodology between soil analysis, Guelph permeameter and rainfall simulations confirmed to be a useful tool to measure these different variations. It is important to highlight the combination of rainfall simulations and Guelph permeameter results to measure the permeability, the infiltration, the runoff and the soil erosion processes, which is not common in the scientific literature (Gupta et al., 2006, 1993; Leonard and Andrieux, 1998). Small portable rainfall simulator could demonstrate the high superficial infiltration, due to the elevated stoniness and roughness (several micro-topographical changes), cracks and high silt content, joined to the constant soil

tillage practices by the farmers and the Guelph permeameter could show a hydrological connectivity on depth showing a decrease of the values between the upper and foot slope. Therefore, this study can contribute as a valuable part of new studies about land degradation of viticulture regions (Corbane et al., 2012; Likar et al., 2015; López-Piñero et al., 2013; Martínez-Casasnovas et al., 2005; Novara et al., 2011; Prosdocimi et al., 2016a; 2016b; Ramos et al., 2015; Rodrigo-Comino et al., 2016a, 2016b; Salome et al., 2014).

Several authors confirmed that the pedological characteristics and human influences are directly connected with a high hydrological and soil erosion variabilities, which generate several intra-plot differences (Arnáez et al., 2007; Follain et al., 2012; Govers, 1985; Govers et al., 1994; Imeson and Lavee, 1998; Novara et al., 2013; Ortigosa and Lasanta 1984; Quiquerez et al., 2014; Ruiz-Sinoga and Martínez-Murillo, 2009a, 2009b). According to this, by using the Guelph permeameter, repeated steady rates and permeability rates were observed during almost all of the experiments, but at the same time the values were different in each of them. Therefore, the final averages cannot show a universal value for the steady rate in the study area, because all the data obtained a high standard deviation. Rodrigo-Comino et al. (2016b) noted the same high variability (with similar pedological and topographical characteristics) after applying the same method in German vineyards with steep slopes. On the upper slope, they obtained $42.5 \pm 44.7 \text{ mm h}^{-1}$, on the middle $20.1 \pm 16.2 \text{ mm h}^{-1}$ and on the foot slope $16.8 \pm 27.4 \text{ mm h}^{-1}$. Therefore, it would be accurate to affirm: i) the existence of different permeability rates along different slope positions and depths or, on the contrary; ii) the several difficulties to find a universal permeability rates with the Guelph permeameter.

Related to the rainfall simulations, the highest values of soil loss and runoff were registered on the upper and foot slope, which showed also more concentration of silt particles and the lowest organic matter content in the soil. On the contrary, in the middle slope with the highest concentration of sand particles and organic matter content, the runoff and soil loss decreased. The importance of the role of the organic matter, the fine textural organisation (Le Bissonnais et al., 1998; Ortigosa and Lasanta 1984; Salome et al., 2014), the soil tillage and the rock fragments (Biddoccu et al., 2013; Follain et al., 2012; Govers et al., 1994; Poesen et al., 1997, 1994) was reflected in these irregularities of the

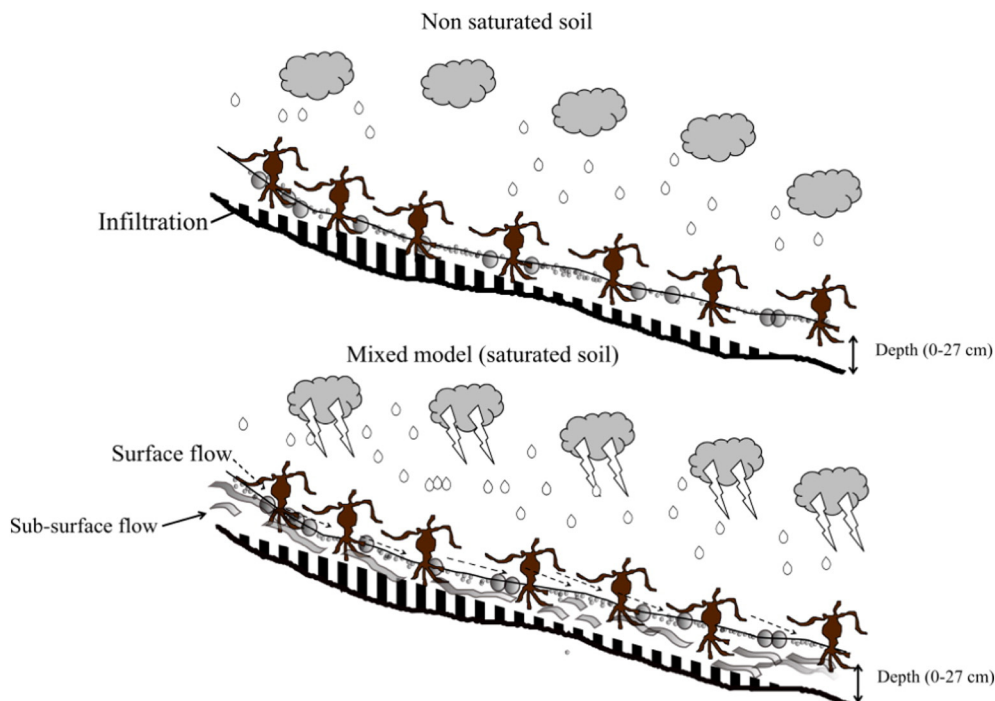


Fig. 6. Runoff generation model under Mediterranean conditions in hillslope vineyards.

spatial distribution of the rainfall simulation results. In the most of cases, runoff activated the soil erosion processes with an increase of the soil loss. In this line, Rodrigo-Comino et al. (2016a), comparing eight European vineyards from France, Germany and Spain, obtained a high correlation between an increase of the SSL and an increase in runoff coefficient (0.607).

To put in a general context the obtained results of this research, we can compare these results with other studies, which have used the same small portable rainfall simulator in other vineyards. For example, Rodrigo-Comino et al. (2015a, 2015b) showed lower average values for German vineyards in Ruwer-Mosel valley with also high infiltration rates and sub-surface processes, a total average runoff of $0.62 \text{ L}^{-1} \text{ m}^{-2}$ and a soil loss of $1.05 \text{ g}^{-1} \text{ m}^{-2}$. These results supposed a high sediment concentration of 6.17 g L^{-1} . On the contrary, different initial soil erosion processes was observed by Rodrigo Comino et al., (2016c), who compared ecological and conventional vineyards in Saar-Mosel valley. For this case, higher runoff ($5.19 \text{ L}^{-1} \text{ m}^{-2}$) and soil loss ($29.67 \text{ g}^{-1} \text{ m}^{-2}$) than in the Montes de Málaga were obtained in the conventional vineyards. However, respect to the ecological vineyards, only $0.48 \text{ L}^{-1} \text{ m}^{-2}$ of runoff and $0.52 \text{ g}^{-1} \text{ m}^{-2}$ were registered. Finally, this research can be compared with other studied, which was carried out in Valencia using barley straw soils. In this study, the runoff ranged $3.52 \text{ L}^{-1} \text{ m}^{-2}$ and the soil loss $20.59 \text{ g}^{-1} \text{ m}^{-2}$ (Prosdociami et al., 2016a, 2016b; Rodrigo-Comino et al., 2016a).

To understand the initial soil erosion processes in this study area, following the investigations carried out in Germany or Spain, it can be observed that one of the most important key factor was the high susceptibility to sealing, caused by raindrop impact (Lassu et al., 2015; Marzen et al., 2015; Montenegro et al., 2013; Xiao et al., 2015) related to the high silt content. In this line, Ramos et al. (2000) confirmed that the elevated silt values, the inexistence of vegetation cover and the high stone cover are able to generate a natural sieving and the consequent transport of the fine material in down slope direction. However, our results indicated the highest silt and total organic carbon contents occurred on middle slopes, contrarily to the traditional soil erosion theory, which expected to find depleted upper and middle slopes and heavily enriched foot slopes. This situation can be due to the high variability of the distribution of the soil surface components, which generates several different micro-topographical situations along the slope modifying its natural behaviour. These geomorphological and hydrological variabilities were represented in the Fig. 6. The irregularities due to the high roughness and the schistosity of the rocks facilitate the weathering of the materials, which acquire a laminar morphology and high angularity. This aspect of the rock fragments can offer greater resistance to move the sediments along the slope and cause high micro-topographical variabilities. So, a possible mixed Hortonian-Hewlettian model, combining surface and sub-surface flow, irregular sediment transport and different impacts of the rainfall on the soil at micro-scale could be possible to obtain (Imeson and Lavee, 1998). The study site showed clear mechanisms of connectivity continuously appears and disappears the infiltration, the surface and the sub-surface flow processes. All together perform a pattern from the upper to the foot slope, which develop a continuous feedback system.

This alteration of the natural hydrological dynamic can carry out environmental problems of solute transport, nutrients and soil losses, slides by piping processes, formation of rills and ephemeral gullies, degradation of the roots and decrease of the productivity (Bienes et al., 2016; Bruggisser et al., 2010; De Baets et al., 2011; Galati et al., 2015; García-Díaz et al., 2016; Martínez-Murillo et al., 2013; Morvan et al., 2014; Novara et al., 2013; Poesen et al., 1997; Richter, 1980). In this line in the future, it would be interesting to look deeper in a relevant high intra-plot temporal variabilities along the inter-rows and rills (Bryan et al., 1989; David et al., 2014; Govers et al., 1994; Poesen et al., 1990; Ramos and Martínez-Casasnovas, 2006; Rodrigo-Comino et al., 2015b; Wirtz et al., 2013, 2010). It would be useful to compare soil erosion and hydrological processes before and after harvesting, between different years and under different rainfall intensities.

5. Conclusions

Differences of hydrological and soil erosion processes have been measured for one study area at three different slope positions in a Spanish viticulture area (Montes de Málaga, Spain).

The main obtained pedological and topographical characteristics of the studied vineyards were: i) steep slopes between 15° and 42° , several tillage signals on the soil profile by the vine grower, high gravel content (between 49% and 64%); ii) silty loam texture with higher sand content between 0 and 5 cm (the highest was registered in the middle), and clay content between 5 and 15 cm; iii) inexistence of vegetation cover; iv) high stone cover and roughness. Due to these parameters several differences of the permeability measured with a Guelph permeameter between slope positions were registered. An increase of the rates was founded from the upper slope to the foot slope. The final averages could not show a universal value for the steady rate in the study area, because all the data obtained a high standard deviation.

On the other hand, applying a small portable rainfall simulator, results did not show the highest soil loss from the upper to the middle slope, contrarily to a natural soil erosion trend. This situation was due to the high variability to the soil surface components, which generate different micro-topographical situations along the slope modifying the natural behaviour through a mixed Hortonian-Hewlettian model. This eco-geomorphological system is sensible to irregular variations of surface and sub-surface flow, sediment transport and different impacts of the rainfall drops on the soil at micro-scale.

Acknowledgements

Firstly, we acknowledge the farmer's syndicate UPA (Unión de Pequeños Agricultores) and the wine-grower Pepe Gámez (Almáchar) for providing access to the study area. Secondly, we thank the students of the Bachelor course and Master from Trier University for their hard efforts in the field and laboratory works in the Almáchar campaign (September, 2015). Thirdly, we acknowledge the geomorphology and soil laboratory technicians María Pedraza and Rubén Rojas of Instituto de Geomorfología y Suelos (Málaga University) for the soil analysis. Furthermore, we thank Cristian Cuevas Zamora for the English corrections.

Finally, we also thank the Caixa-Bank and DAAD (Deutscher Akademischer Austauschdienst) for the Scholarship grant awarded to J. Rodrigo Comino.

References

- Aguilar-Ruiz, J., et al., 1993. Mapa de suelos; hoja 1053-1067 (Málaga-Torremolinos) escala 1:100000. LUCDEME. Granada University, Spain.
- Archer, N.A.L., Bonell, M., Coles, N., MacDonald, A.M., Auton, C.A., Stevenson, R., 2013. Soil characteristics and land cover relationships on soil hydraulic conductivity at a hill-slope scale: a view towards local flood management. *J. Hydrol.* 497, 208–222. <http://dx.doi.org/10.1016/j.jhydrol.2013.05.043>.
- Arnáez, J., Lasanta, T., Ruiz-Flaño, P., Ortigosa, L., 2007. Factors affecting runoff and erosion under simulated rainfall in Mediterranean vineyards. *Soil Tillage Res.* 93, 324–334. <http://dx.doi.org/10.1016/j.still.2006.05.013>.
- Bagarello, V., Castellini, M., Di Prima, S., Iovino, M., 2014. Soil hydraulic properties determined by infiltration experiments and different heights of water pouring. *Geoderma* 213, 492–501. <http://dx.doi.org/10.1016/j.geoderma.2013.08.032>.
- Biddocci, M., Ferraris, S., Cavallo, E., Opsi, F., Previati, M., Canone, D., 2013. Hillslope vineyard rainfall-runoff measurements in relation to soil infiltration and water content. *Procedia Environ. Sci.*, Four decades of progress in monitoring and modeling of processes in the soil-plant-atmosphere system: applications and challenges. 19, 351–360. <http://dx.doi.org/10.1016/j.proenv.2013.06.040>.
- Bienes, R., Marqués, M.J., Sastre, B., García-Díaz, A., Ruiz-Colmenero, M., 2016. Eleven years after shrub revegetation in semiarid eroded soils. Influence in soil properties. *Geoderma* 273, 106–114. <http://dx.doi.org/10.1016/j.geoderma.2016.03.023>.
- Blanco-Sepúlveda, R., Gómez-Moreno, M.L., 2006. Agua y sociedad rural en los montes de Málaga: sistemas hidráulicos en el hábitat disperso del s. XIX. *Baética Estud. Arte Geogr. E Hist.* 28, 259–282.
- Blanco-Sepúlveda, R., Larrubia-Vargas, R., 2008. Usos agrarios y sostenibilidad medioambiental. Evaluación de la capacidad agrológica y socioeconómica de la Axarquía (Málaga). *Cuad. Geol. Univ. Granada* 42, 83–108.
- Blanco-Sepúlveda, R., Senciales-González, J.M., 2001a. La influencia de los factores formadores en las variaciones de las características y propiedades de los suelos de los montes de Málaga. *Baética Estud. Arte Geogr. E Hist.* 23, 9–24.

- Blanco-Sepúlveda, R., Senciales-González, J.M., 2001b. Factores edáficos diferenciadores en suelos reforestados: El caso de los montes de Málaga. *Baética Estud. Arte Geogr. E Hist.* 23, 193–220.
- Bodhinayake, W., Cheng Si, B., 2004. Near-saturated surface soil hydraulic properties under different land uses in the St Denis National Wildlife Area, Saskatchewan, Canada. *Hydrol. Process.* 18, 2835–2850. <http://dx.doi.org/10.1002/hyp.1497>.
- Bruggisser, O.T., Schmidt-Entling, M.H., Bacher, S., 2010. Effects of vineyard management on biodiversity at three trophic levels. *Biol. Conserv.* 143, 1521–1528. <http://dx.doi.org/10.1016/j.biocon.2010.03.034>.
- Bryan, R.B., Govers, G., Poesen, J., 1989. The concept of soil erodibility and some problems of assessment and application. Selected papers of the Fourth Benelux Colloquium on Geomorphological Processes. *Catena* 16, 393–412. [http://dx.doi.org/10.1016/0341-8162\(89\)90023-4](http://dx.doi.org/10.1016/0341-8162(89)90023-4).
- Buczko, U., Bens, O., Hüttl, R.F., 2006. Tillage effects on hydraulic properties and macroporosity in silty and sandy soils. *Soil Sci. Soc. Am. J.* 70. <http://dx.doi.org/10.2136/sssaj2006.0046>.
- Cerdà, A., 1999. Simuladores de lluvia y su aplicación a la Geomorfología: Estado de la cuestión. *Cuad. Investig. Geográfica* 25, 45–84.
- Cerdà, A., 1998a. Effect of climate on surface flow along a climatological gradient in Israel: a field rainfall simulation approach. *J. Arid Environ.* 38, 145–159. <http://dx.doi.org/10.1006/jare.1997.0342>.
- Cerdà, A., 1998b. Relationships between climate and soil hydrological and erosional characteristics along climatic gradients in Mediterranean limestone areas. *Geomorphology* 25, 123–134. [http://dx.doi.org/10.1016/S0169-555X\(98\)00033-6](http://dx.doi.org/10.1016/S0169-555X(98)00033-6).
- Cerdà, A., 1997. Soil erosion after land abandonment in a semi-arid environment of south-eastern Spain. *Arid Soil Res. Rehabil.* 11, 163–176. <http://dx.doi.org/10.1080/15324989709381469>.
- Corbane, C., Jacob, F., Raclot, D., Albergel, J., Andrieux, P., 2012. Multitemporal analysis of hydrological soil surface characteristics using aerial photos: a case study on a Mediterranean vineyard. *Int. J. Appl. Earth Obs. Geoinf.* 18, 356–367. <http://dx.doi.org/10.1016/j.jag.2012.03.009>.
- David, M., Follain, S., Ciampalini, R., Le Bissonnais, Y., Couturier, A., Walter, C., 2014. Simulation of medium-term soil redistributions for different land use and landscape design scenarios within a vineyard landscape in Mediterranean France. *Geomorphology* 214, 10–21. <http://dx.doi.org/10.1016/j.geomorph.2014.03.016>.
- Davies, B.E., 1974. Loss-on-ignition as an estimate of soil organic matter 1. *Soil Sci. Soc. Am. J.* 38. <http://dx.doi.org/10.2136/sssaj1974.03615995003800010046x>.
- De Baets, S., Poesen, J., Meersmans, J., Serlet, L., 2011. Cover crops and their erosion-reducing effects during concentrated flow erosion. *Catena* 85, 237–244. <http://dx.doi.org/10.1016/j.catena.2011.01.009>.
- Elrick, D.E., Reynolds, W.D., Tan, K.A., 1989. Hydraulic conductivity measurements in the unsaturated zone using improved well analyses. *Ground Water Monit. Remediat.* 9, 184–193. <http://dx.doi.org/10.1111/j.1745-6592.1989.tb01162.x>.
- Elrick, D.E., Reynolds, W.D., 1992. Methods for analyzing constant-head well permeameter data. *Soil Sci. Soc. Am. J.* 56, 320–323. <http://dx.doi.org/10.2136/sssaj1992.03615995005600010052x>.
- Estévez-González, C., Chamón, C., 1978. Mapa Geológico y memoria explicativa de la Hoja de Málaga-Torremolinos (1.053-1067), 1:50,000.
- Follain, S., Ciampalini, R., Crabit, A., Coulouma, G., Garnier, F., 2012. Effects of redistribution processes on rock fragment variability within a vineyard topsoil in Mediterranean France. *Geomorphology* 175–176, 45–53. <http://dx.doi.org/10.1016/j.geomorph.2012.06.017>.
- Galati, A., Gristina, L., Crescimanno, M., Barone, E., Novara, A., 2015. Towards more efficient incentives for agri-environment measures in degraded and eroded vineyards. *Land Degrad. Dev.* 26, 557–564. <http://dx.doi.org/10.1002/ldr.2389>.
- García-Díaz, A., Allas, R.B., Gristina, L., Cerdà, A., Pereira, P., Novara, A., 2016. Carbon input threshold for soil carbon budget optimization in eroding vineyards. *Geoderma* 271, 144–149. <http://dx.doi.org/10.1016/j.geoderma.2016.02.020>.
- Govers, G., 1985. Selectivity and transport capacity of thin flows in relation to rill erosion. *Catena* 12, 35–49. [http://dx.doi.org/10.1016/S0341-8162\(85\)80003-5](http://dx.doi.org/10.1016/S0341-8162(85)80003-5).
- Govers, G., Vandaele, K., Desmet, P., Poesen, J., Bunte, K., 1994. The role of tillage in soil redistribution on hillslopes. *Eur. J. Soil Sci.* 45, 469–478. <http://dx.doi.org/10.1111/j.1365-2389.1994.tb00532.x>.
- Gruber, B., Kosegarten, H., 2002. Depressed growth of non-chlorotic vine grown in calcareous soil is an iron deficiency symptom prior to leaf chlorosis. *J. Plant Nutr. Soil Sci.* 165, 111–117. [http://dx.doi.org/10.1002/1522-2624\(200202\)165:1<111::AID-JPLN111>3.0.CO;2-B](http://dx.doi.org/10.1002/1522-2624(200202)165:1<111::AID-JPLN111>3.0.CO;2-B).
- Gupta, R.K., Rudra, R.P., Dickinson, W.T., Patni, N.K., Wall, G.J., 1993. Comparison of saturated hydraulic conductivity measured by various field methods. *Trans. ASAE* 36, 51–55. <http://dx.doi.org/10.13031/2013.28313>.
- Gupta, R.K., Rudra, R.P., Parkin, G., 2006. Analysis of spatial variability of hydraulic conductivity at field scale. *Can. Biosyst. Eng.* 48, 1.55–1.62.
- Gwenzl, W., Hinz, C., Holmes, K., Phillips, I.R., Mullins, I.J., 2011. Field-scale spatial variability of saturated hydraulic conductivity on a recently constructed artificial ecosystem. *Geoderma* 166, 43–56. <http://dx.doi.org/10.1016/j.geoderma.2011.06.010>.
- Haba, J.P., 1997. La exportación de vino de España. Los efectos de la integración en la Unión Europea. *Cuad. Geogr.* 61, 117–143.
- Huang, M., Rodger, H., Barbour, S.L., 2014. An evaluation of air permeability measurements to characterize the saturated hydraulic conductivity of soil reclamation covers. *Can. J. Soil Sci.* 95, 15–26. <http://dx.doi.org/10.4141/cjss-2014-072>.
- Huang, M., Zettl, J.D., Lee Barbour, S., Pratt, D., 2016. Characterizing the spatial variability of the hydraulic conductivity of reclamation soils using air permeability. *Geoderma* 262, 285–293. <http://dx.doi.org/10.1016/j.geoderma.2015.08.014>.
- Imeson, A.C., Lavee, H., 1998. Soil erosion and climate change: the transect approach and the influence of scale. *Geomorphology* 23, 219–227. [http://dx.doi.org/10.1016/S0169-555X\(98\)00005-1](http://dx.doi.org/10.1016/S0169-555X(98)00005-1).
- Iserloh, T., Fister, W., Seeger, M., Willger, H., Ries, J.B., 2012. A small portable rainfall simulator for reproducible experiments on soil erosion. *Soil Tillage Res.* 124, 131–137. <http://dx.doi.org/10.1016/j.still.2012.05.016>.
- Iserloh, T., Ries, J.B., Arnáez, J., Boix-Fayos, C., Butzen, V., Cerdà, A., Echeverría, M.T., Fernández-Gálvez, J., Fister, W., Geißler, C., Gómez, J.A., Gómez-Macpherson, H., Kuhn, N.J., Lázaro, R., León, F.J., Martínez-Mena, M., Martínez-Murillo, J.F., Marzen, M., Mingorance, M.D., Ortigosa, L., Peters, P., Regüés, D., Ruiz-Sinoga, J.D., Scholten, T., Seeger, M., Solé-Benet, A., Wengel, R., Wirtz, S., 2013a. European small portable rainfall simulators: a comparison of rainfall characteristics. *Catena* 110, 100–112. <http://dx.doi.org/10.1016/j.catena.2013.05.013>.
- Iserloh, T., Ries, J.B., Cerdà, A., Echeverría, M.T., Fister, W., Geissler, C., Kuhn, N.J., León, F.J., Peters, P., Schindewolf, M., Schmidt, J., Scholten, T., Seeger, M., 2013b. Comparative measurements with seven rainfall simulators on uniform bare fallow land. *Z. Für Geomorphol. Suppl.* 57, 11–26.
- IUSS Working Group WRB, 2014. World Reference Base for Soil Resources, World Soil Resources Report. FAO, Rome.
- IUSS Working Group WRB, 2007. Land Evaluation. Towards a Revised Framework. second ed. Land and Water discussion paper. FAO, Rome.
- IUSS Working Group WRB, 2006. Guidelines for Constructing Small Scale Map Legends Using the WRB. second ed. World Soil Resources. FAO, Rome.
- Jačka, L., Pavlásek, J., Kuráž, V., Pech, P., 2014. A comparison of three measuring methods for estimating the saturated hydraulic conductivity in the shallow subsurface layer of mountain podzols. *Geoderma* 219–220, 82–88. <http://dx.doi.org/10.1016/j.geoderma.2013.12.027>.
- Jackson, R.S., 2014. Wine science. Principles and Applications, fourth ed. Elsevier, London.
- Justicia Segovia, A., 1988. Problemática estructural de la Población en la Montaña Malagueña. *Baética Estud. Arte Geogr. E Hist.* 11, 15–40.
- Kodešová, R., Šimunek, J., Nikodem, A., Jirků, V., 2010. Estimation of the dual-permeability model parameters using tension disk infiltrometer and Guelph permeameter all rights reserved. No part of this periodical may be reproduced or transmitted in any form or by any means, electronic or mechanical, including photocopying, recording, or any information storage and retrieval system, without permission in writing from the publisher. *J. 9 Vadose Zone* <http://dx.doi.org/10.2136/vzj2009.0069>.
- Kumar, S., Sekhar, M., Reddy, D.V., Mohan Kumar, M.S., 2010. Estimation of soil hydraulic properties and their uncertainty: comparison between laboratory and field experiment. *Hydrol. Process.* 24, 3426–3435. <http://dx.doi.org/10.1002/hyp.7775>.
- Lasanta, T., García-Ruiz, J.M., Pérez-Rontomé, C., Sancho-Marcén, C., 2000. Runoff and sediment yield in a semi-arid environment: the effect of land management after farmland abandonment. *Catena* 38, 265–278. [http://dx.doi.org/10.1016/S0341-8162\(99\)00079-X](http://dx.doi.org/10.1016/S0341-8162(99)00079-X).
- Lassu, T., Seeger, M., Peters, P., Keesstra, S.D., 2015. The Wageningen rainfall simulator: set-up and calibration of an indoor nozzle-type rainfall simulator for soil erosion studies. *Land Degrad. Dev.* 26, 604–612. <http://dx.doi.org/10.1002/ldr.2360>.
- Le Bissonnais, Y., Benkhadra, H., Chaplot, V., Fox, D., King, D., Daroussin, J., 1998. Crusting, runoff and sheet erosion on silty loamy soils at various scales and upscaling from m² to small catchments. *Soil Tillage Res.* 46, 69–80. [http://dx.doi.org/10.1016/S0167-1987\(98\)80109-8](http://dx.doi.org/10.1016/S0167-1987(98)80109-8).
- Leonard, J., Andrieux, P., 1998. Infiltration characteristics of soils in Mediterranean vineyards in Southern France. *Catena* 32, 209–223. [http://dx.doi.org/10.1016/S0341-8162\(98\)00049-6](http://dx.doi.org/10.1016/S0341-8162(98)00049-6).
- Lesch, S.M., Corwin, D.L., 2003. Using the dual-pathway parallel conductance model to determine how different soil properties influence conductivity survey data. *Agron. J.* 95, 365–379. <http://dx.doi.org/10.2134/agronj2003.3650>.
- Likar, M., Vogel-Mikuš, K., Potisek, M., Hančević, K., Radič, T., Nečemer, M., Regvar, M., 2015. Importance of soil and vineyard management in the determination of grapevine mineral composition. *Sci. Total Environ.* 505, 724–731. <http://dx.doi.org/10.1016/j.scitotenv.2014.10.057>.
- López-Piñero, A., Muñoz, A., Zamora, E., Ramírez, M., 2013. Influence of the management regime and phenological state of the vines on the physicochemical properties and the seasonal fluctuations of the microorganisms in a vineyard soil under semi-arid conditions. *Soil Tillage Res.* 126, 119–126. <http://dx.doi.org/10.1016/j.still.2012.09.007>.
- MacDonald, A.M., Maurice, L., Dobbs, M.R., Reeves, H.J., Auton, C.A., 2012. Relating in situ hydraulic conductivity, particle size and relative density of superficial deposits in a heterogeneous catchment. *J. Hydrol.* 434–435, 130–141. <http://dx.doi.org/10.1016/j.jhydrol.2012.01.018>.
- Martínez-Murillo, J.F., Senciales-González, J.M., 2003. Morfogénesis y procesos edáficos: el Caso de los Montes de Málaga. *Baética Estud. Arte Geogr. E Hist.* 25, 219–258.
- Martínez-Casasnovas, J.A., Ramos, M.C., Ribes-Dasi, M., 2005. On-site effects of concentrated flow erosion in vineyard fields: some economic implications. *Catena* 60, 129–146. <http://dx.doi.org/10.1016/j.catena.2004.11.006>.
- Martínez-Murillo, J.F., Nadal-Romero, E., Regüés, D., Cerdà, A., Poesen, J., 2013. Soil erosion and hydrology of the western Mediterranean badlands throughout rainfall simulation experiments: a review, updating badlands research. *Catena* 106, 101–112. <http://dx.doi.org/10.1016/j.catena.2012.06.001>.
- Marzen, M., Iserloh, T., Casper, M.C., Ries, J.B., 2015. Quantification of particle detachment by rain splash and wind-driven rain splash. *Catena* 127, 135–141. <http://dx.doi.org/10.1016/j.catena.2014.12.023>.
- Montenegro, A.A.A., Abrantes, J.R.C.B., de Lima, J.L.M.P., Singh, V.P., Santos, T.E.M., 2013. Impact of mulching on soil and water dynamics under intermittent simulated rainfall. *Catena* 109, 139–149. <http://dx.doi.org/10.1016/j.catena.2013.03.018>.
- Morvan, X., Naisse, C., Malam Issa, O., Desprats, J.F., Combaud, A., Cerdan, O., 2014. Effect of ground-cover type on surface runoff and subsequent soil erosion in champagne vineyards in France. *Soil Use Manag.* 30, 372–381. <http://dx.doi.org/10.1111/sum.12129>.

- Novara, A., Gristina, L., Guaitoli, F., Santoro, A., Cerdà, A., 2013. Managing soil nitrate with cover crops and buffer strips in Sicilian vineyards. *Solid Earth* 4, 255–262. <http://dx.doi.org/10.5194/se-4-255-2013>.
- Novara, A., Gristina, L., Saladino, S.S., Santoro, A., Cerdà, A., 2011. Soil erosion assessment on tillage and alternative soil managements in a Sicilian vineyard. *Soil Tillage Res.* 117, 140–147. <http://dx.doi.org/10.1016/j.still.2011.09.007>.
- Ortigosa, L.M., Lasanta, T., 1984. El papel de la escorrentía en la organización textural de suelos cultivados en pendiente: modelos en viñedos de La Rioja. *Cuad. Investig. Geográfica* 10, 99–112.
- Padilla-Monge, A., 2001. Comercio y comerciantes en la historia antigua de Málaga : (siglo VIII a.C.-año 711 a.C.). II Congreso de Historia Antigua de Málaga. Málaga, Spain, pp. 385–418.
- Peter, K.D., Ries, J.B., 2013. Infiltration rates affected by land levelling measures in the Souss valley, South Morocco. *Z. Für Geomorphol.* 57, 59–72.
- Poesen, J., Ingelmo-Sanchez, F., Mucher, H., 1990. The hydrological response of soil surfaces to rainfall as affected by cover and position of rock fragments in the top layer. *Earth Surf. Process. Landf.* 15, 653–671. <http://dx.doi.org/10.1002/esp.3290150707>.
- Poesen, J., Van Wesemael, B., Govers, G., Martínez-Fernández, J., Desmet, P., Vandaele, K., Quine, T., Degraer, G., 1997. Patterns of rock fragment cover generated by tillage erosion. *Geomorphology* 18, 183–197.
- Poesen, J.W., Torri, D., Bunte, K., 1994. Effects of rock fragments on soil erosion by water at different spatial scales: a review. *Catena* 23, 141–166. [http://dx.doi.org/10.1016/0341-8162\(94\)90058-2](http://dx.doi.org/10.1016/0341-8162(94)90058-2).
- Prosdocimi, M., Cerdà, A., Tarolli, P., 2016a. Soil water erosion on Mediterranean vineyards: a review. *Catena* 141, 1–21. <http://dx.doi.org/10.1016/j.catena.2016.02.010>.
- Prosdocimi, M., Jordán, A., Tarolli, P., Keesstra, S., Novara, A., Cerdà, A., 2016b. The immediate effectiveness of barley straw mulch in reducing soil erodibility and surface runoff generation in Mediterranean vineyards. *Sci. Total Environ.* 547, 323–330. <http://dx.doi.org/10.1016/j.scitotenv.2015.12.076>.
- Quintana-Toret, F.J., 1985. Los orígenes Históricos de la Viticultura Malagueña. *Baética Estud. Arte Geogr. E Hist.* 8, 393–404.
- Quiquerez, A., Chevigny, E., Allemand, P., Curmi, P., Petit, C., Grandjean, P., 2014. Assessing the impact of soil surface characteristics on vineyard erosion from very high spatial resolution aerial images (Côte de Beaune, Burgundy, France). *Catena* 116, 163–172. <http://dx.doi.org/10.1016/j.catena.2013.12.002>.
- Ramos, M.C., Benito, C., Martínez-Casasnovas, J.A., 2015. Simulating soil conservation measures to control soil and nutrient losses in a small, vineyard dominated, basin. *Agric. Ecosyst. Environ.* 213, 194–208. <http://dx.doi.org/10.1016/j.agee.2015.08.004>.
- Ramos, M.C., Martínez-Casasnovas, J.A., 2006. Impact of land levelling on soil moisture and runoff variability in vineyards under different rainfall distributions in a Mediterranean climate and its influence on crop productivity. *J. Hydrol.* 321, 131–146. <http://dx.doi.org/10.1016/j.jhydrol.2005.07.055>.
- Ramos, M.C., Nacci, S., Pla, I., 2000. Soil sealing and its influence on erosion rates for some soils in the Mediterranean area. *Soil Sci.* 165, 398–403.
- Reynolds, W.D., 1986. The Guelph Permeameter Method for in situ Measurement of Field-Saturated Hydraulic Conductivity and Matric Flux Potential. University of Guelph, Guelph, Ontario, Canada.
- Reynolds, W.D., Elrick, D.E., 2002. Constant head well permeameter (vadose zone). In: Dane, J.H., Topp, G.C. (Eds.), *Methods of soil analysis, Physical Methods*. Soil Science Society of America, Inc., Madison, WI (USA), pp. 844–858.
- Reynolds, W.D., Elrick, D.E., 1987. A laboratory and numerical assessment of the Guelph permeameter method. *Soil Sci.* 144, 282–299.
- Reynolds, W.D., Lewis, J.K., 2012. A drive point application of the Guelph permeameter method for coarse-textured soils. *Geoderma* 187–188, 59–66. <http://dx.doi.org/10.1016/j.geoderma.2012.04.004>.
- Richter, G., 1980. On the soil erosion problem in the temperate humid area of Central Europe. *Geojournal* 4, 279–287.
- Rienznier, M., Gandolfi, C., 2014. Investigation of spatial and temporal variability of saturated soil hydraulic conductivity at the field-scale. *Soil Tillage Res.* 135, 28–40. <http://dx.doi.org/10.1016/j.still.2013.08.012>.
- Ries, J.B., Seeger, M., Iserloh, T., Wistorf, S., Fister, W., 2009. Calibration of simulated rainfall characteristics for the study of soil erosion on agricultural land. *Soil Tillage Res.* 106, 109–116. <http://dx.doi.org/10.1016/j.still.2009.07.005>.
- Rodrigo-Comino, J., 2014. Los suelos de la provincia de Málaga: revisión y actualización de las fuentes edafológicas según la clasificación de FAO-WRB. Servicio de Publicaciones y Divulgación Científica. Universidad de Málaga, Málaga.
- Rodrigo-Comino, J., Brings, C., Lassu, T., Iserloh, T., Senciales, J., Martínez-Murillo, J., Ruiz-Sinoga, J., Seeger, M., Ries, J.B., 2015a. Rainfall and human activity impacts on soil losses and rill erosion in vineyards (Ruwer Valley, Germany). *Solid Earth* 6, 823–837. <http://dx.doi.org/10.5194/se-6-823-2015>.
- Rodrigo-Comino, J., Iserloh, T., Morvan, X., Malam-Issa, O., Naisse, C., Keesstra, S.D., Cerdà, A., Prosdocimi, M., Arnáez, J., Lasanta, T., Ramos, M.C., Marqués, M.J., Ruiz-Colmenero, M., Bienes, R., Ruiz-Sinoga, J.D., Seeger, M., Ries, J.B., 2016a. Soil erosion processes in European vineyards: a qualitative comparison of rainfall simulation measurements in Germany, Spain and France. *Hydrology* 3, 6. <http://dx.doi.org/10.3390/hydrology3010006>.
- Rodrigo-Comino, J., Lassu, T., Senciales-González, J.M., Ruiz-Sinoga, J.D.R., Seeger, M., Ries, J.B., 2015b. Estudio de procesos geomorfológicos en campos cultivados de viñedos sobre laderas en pendientes en el valle del Ruwer (Alemania). *Cuad. Geográficos* 54, 6–26.
- Rodrigo-Comino, J., Seeger, M., Senciales-González, J.M., Ruiz-Sinoga, J.D., Ries, J.B., 2016b. Variación espacio-temporal de los procesos hidrológicos del suelo en viñedos con elevadas pendientes (Valle del Ruwer-Mosela, Alemania). *Cuad. Investig. Geográfica* 42. <http://dx.doi.org/10.18172/cig.2934> (In press).
- Rodrigo Comino, J., Iserloh, T., Lassu, T., Cerdà, A., Keesstra, S.D., Prosdocimi, M., Brings, C., Marzen, M., Ramos, M.C., Senciales, J.M., Ruiz-Sinoga, J.D., Seeger, M., Ries, J.B., 2016. Quantitative comparison of initial soil erosion processes and runoff generation in Spanish and German vineyards. *Sci. Total Environ.* <http://dx.doi.org/10.1016/j.scitotenv.2016.05.163>.
- Rodrigo-Comino, J., Senciales-González, J.M., 2015. Ratio LE para el ajuste de perfiles longitudinales en cursos fluviales de montaña. Aplicación a la cuenca del río Almáchar (Málaga, España). *Cuaternario Geomorfol.* 29, 31–56.
- Rosell, R.A., Gasparoni, J.C., Galantini, J.A., 2001. Soil organic matter evaluation. In: Lal, R., Kimble, J., Follet, R., Stewart, B. (Eds.), *Assessment methods for soil carbon*. Lewis Publishers, USA, pp. 311–322.
- Ruiz-Sinoga, J.D., 1987. Influencia del medio físico sobre el viñedo en las Cordilleras Béticas litorales. *An. Geogr. Univ. Complut.* 7, 315–323.
- Ruiz-Sinoga, J.D., García-Marín, R., Martínez-Murillo, J.F., Gabarrón-Galeote, M.A., 2011. Precipitation dynamics in southern Spain: trends and cycles. *Int. J. Climatol.* 31, 2281–2289. <http://dx.doi.org/10.1002/joc.2235>.
- Ruiz-Sinoga, J.D., García-Marín, R., Martínez-Murillo, J.F., Gabarrón-Galeote, M.A., 2010. Pluviometric gradient incidence and the hydrological behaviour of soil surface components (southern Spain). *Land Degrad. Dev.* 21, 484–495. <http://dx.doi.org/10.1002/ldr.994>.
- Ruiz-Sinoga, J.D., Martínez-Murillo, J.F., 2009a. Hydrological response of abandoned agricultural soils along a climatological gradient on metamorphic parent material in southern Spain. *Earth Surf. Process. Landf.* 34, 2047–2056. <http://dx.doi.org/10.1002/esp.1890>.
- Ruiz-Sinoga, J.D., Martínez-Murillo, J.F., 2009b. Effects of soil surface components on soil hydrological behaviour in a dry Mediterranean environment (Southern Spain). *Geomorphology* 108, 234–245. <http://dx.doi.org/10.1016/j.geomorph.2009.01.012>.
- Ruiz-Sinoga, J.D., Romero-Díaz, A., 2010. Soil degradation factors along a Mediterranean pluviometric gradient in Southern Spain. *Geomorphology* 118, 359–368. <http://dx.doi.org/10.1016/j.geomorph.2010.02.003>.
- Saleh, A., 1993. Soil roughness measurement: chain method. *J. Soil Water Conserv.* 48, 527–529.
- Salome, C., Coll, P., Lardo, E., Villenave, C., Blanchart, E., Hinsinger, P., Marsden, C., Le Cadre, E., 2014. Relevance of use-invariant soil properties to assess soil quality of vulnerable ecosystems: the case of Mediterranean vineyards. *Ecol. Indic.* 43, 83–93. <http://dx.doi.org/10.1016/j.ecolind.2014.02.016>.
- Senciales González, J.M., Rodrigo Comino, J., 2011. Geomorfología de los Montes de Málaga: pasado, presente y ¿futuro? *Baética Estud. Arte Geogr. E Hist.* 33, 81–110.
- Soil moisture Equipment Corp., 2008. Model 2800 K1 Guelph Permeameter Operating Instructions, Soil Moisture Equipment Corp. ed. Santa Barbara, USA.
- Taylor, J.A., Coulouma, G., Lagacherie, P., Tisseyre, B., 2009. Mapping soil units within a vineyard using statistics associated with high-resolution apparent soil electrical conductivity data and factorial discriminant analysis. *Geoderma* 153, 278–284. <http://dx.doi.org/10.1016/j.geoderma.2009.08.014>.
- Vaudour, E., Costantini, E., Jones, G.V., Mocali, S., 2015. An overview of the recent approaches to terroir functional modelling, footprinting and zoning. *SOIL* 1, 287–312. <http://dx.doi.org/10.5194/soil-1-287-2015>.
- Wirtz, S., Seeger, M., Ries, J.B., 2010. The rill experiment as a method to approach a quantification of rill erosion process activity. *Z. Für Geomorphol. NF* 54, 47–64.
- Wirtz, S., Seeger, M., Zell, A., Wagner, C., Wagner, J.-F., Ries, J.B., 2013. Applicability of different hydraulic parameters to describe soil detachment in eroding rills. *PLoS One* 8, 1–11. <http://dx.doi.org/10.1371/journal.pone.0064861>.
- Wu, L., Swan, J.B., Paulson, W.H., Randall, G.W., 1992. Tillage effects on measured soil hydraulic properties. *Soil Tillage Res.* 25, 17–33. [http://dx.doi.org/10.1016/0167-1987\(92\)90059-K](http://dx.doi.org/10.1016/0167-1987(92)90059-K).
- Xiao, L., Hu, Y., Greenwood, P., Kuhn, N.J., 2015. A combined raindrop aggregate destruction test-settling tube (RADT-ST) approach to identify the settling velocity of sediment. *Hydrology* 2, 176. <http://dx.doi.org/10.3390/hydrology2040176>.
- Zhang, Z.F., Groenevelt, P.H., Parkin, G.W., 1998. The well-shape factor for the measurement of soil hydraulic properties using the Guelph permeameter. *Soil Tillage Res.* 49, 219–221. [http://dx.doi.org/10.1016/S0167-1987\(98\)00174-3](http://dx.doi.org/10.1016/S0167-1987(98)00174-3).